

REACTIVE WETTING OF AN IRON-BASED SUPERALLOY MSA2020 AND 316L STAINLESS STEEL BY MOLTEN ZINC ALLOY

Jing Xu¹, Xingbo Liu¹, Mark A Bright², James G Hemrick³, Ever Barbero¹

¹Mechanical & Aerospace Engineering Department, West Virginia University, Morgantown, WV 26506, USA

²Pyrotek Incorporated, Metallurgy Systems Division, Solon, OH 44139, USA

³Materials Science and Technology Division, Oak Ridge National Laboratory, Oak Ridge, TN 37831, USA

ABSTRACT

The reactive wetting behaviors of MSA2020, an Fe-based superalloy and 316L stainless steel in contact with a molten galvanizing (GI) alloy were investigated by the sessile drop method. The tests were conducted in purified Ar-4% H₂ atmosphere at three temperatures (465°C, 485°C, and 500°C). The contact angle and drop geometry were monitored and the wetting properties were compared between 316L stainless steel and cast MSA2020. Metallographic and chemical analyses were conducted on tested samples to characterize the wetting reactions. It was found that 316L, not only suffered considerable wetting, but also reacted with the molten zinc at a higher rate than MSA2020. As expected, increased temperature accelerated the reaction rates with the molten zinc. The results of this investigation indicated that MSA2020 may potentially be utilized as a new material for submerged pot hardware in continuous galvanizing operations.

Keywords: galvanizing, wetting, sessile drop, MSA2020, 316L

1 INTRODUCTION

Corrosion and erosion of pot hardware by molten zinc have long been an issue of concern in the galvanizing processing industry^(1, 2, 3). The formation of intermetallic phases by reaction between the metallic hardware and galvanizing media aggravates the dross build-up on the pot rolls and bearings, reducing the service life of the pot hardware. The wettability of solids by liquid metals at high temperature carries important implications of interfacial reaction mechanisms for liquid/solid contact⁽⁴⁾. The reactive wetting behaviors of steels in molten zinc and aluminum baths have been well examined by attempts to evaluate the effectiveness of the galvanizing processes. For galvanizing of high strength steel in molten zinc, a study by Bordignon indicated selective oxidation of segregated Mn and Si at 800°C during annealing before hot dipping reduced wettability and reactivity of molten zinc and aluminum on free iron at 460°C⁽⁵⁾. Through similar research project, Giorgi, et al. further pointed out the variance of selective oxidation from segregated constituents as a result of inconsistencies in annealing time and temperature and the consequential impact on reactive wetting, as determined by sessile drop measurements⁽⁶⁾.

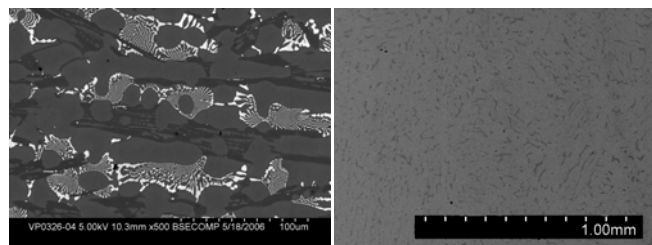
On the other hand, studies of the reaction of alloy materials with molten zinc have been carried out in terms of analysis of weight loss and dimensional changes⁽⁷⁾. However, few reports have previously identified the initial development of the reaction characteristics of superalloys in terms of reactive wetting, which is important in understanding the reactivity of superalloys during actual service conditions. Hence, a need exists for an in-depth investigation on the incipient liquid/solid contact stage by molten zinc through a detailed wetting study. In this paper, work was described on a comparative study of reactive wetting behaviors between 316L stainless steel and an Fe-based superalloy, MSA2020 with molten zinc. The initiation of the reaction process and the reactivity of these materials were examined by analyzing contact angles and droplet geometry. Evolution of the liquid/solid reaction was further explored by conducting compositional and structural analysis on the interfacial reaction layers. The results provide fundamental insight into the understanding of the reaction mechanisms of superalloy materials in a molten zinc bath and facilitate optimization and application of MSA2020 as a bath hardware material for the galvanizing industry.

2 EXPERIMENTAL

316L stainless steel and MSA2020 (the Fe-based, carbide-rich superalloy supplied by Metallurgy Systems Division of Pyrotek Inc.) were studied as the substrate materials in this wetting investigation. The as-cast MSA2020 contained a continuous network of interpenetrating microscopic intermetallic phases and solid solution metallic phases. The presence of metallic phases provided significant improvement in toughness and damage tolerance, while the intermetallic phases contributed to high hardness and improved performance at elevated temperatures. The microstructures of the substrates, MSA2020 superalloy and 316L stainless steel, are shown in Figures 1(a) and 1(b), respectively. As can be seen in Figure 1(a), MSA2020 consisted of distinct primary dendrites of a Mo/W-containing intermetallic phase as well as a Cr-enriched intermetallic phase bound together with a network of eutectic solid solution phase matrix.

Galvanizing zinc alloy samples which contained 0.23 wt. %Al were machined down to cubes (5 mm × 5 mm × 3 mm) for melting during static wetting tests and also extruded into wire segments of 3 mm diameter to produce molten

sessile drops during dynamic testing. Experiments were carried out at various temperatures from 465°C to 500°C and different testing duration from 1 to 4 hours.



(a) (b)
Figure 1: Microstructure of the tested samples:
(a) MSA2020 (b) 316L

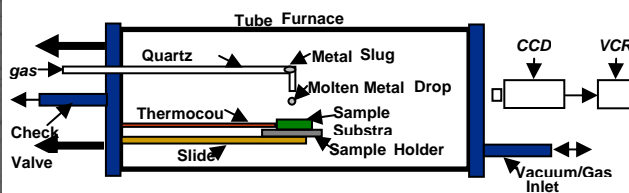


Figure 2: Schematic overview of the sessile drop unit

Both static and dynamic sessile drop methods were employed for studying the wettability. The apparatus used for both methods of sessile drop experiments is schematically illustrated in Figure 2 and consisted of a 33 kW horizontal circular infrared furnace fitted with a rotary pump evacuating system and continuous gas system. A small diameter quartz tube was also passed through the copper lid and extended to a location directly above the sample substrate where the tube was bent 90° and its diameter was reduced. This tube was used to contain the zinc alloy wire segment during heating and melting which produced the molten metal drop for the dynamic tests. Both sealed end caps of the furnace assembly contained quartz windows allowing a high resolution color CCD camera to monitor the experiments. Three Type-S thermocouples (with ceramic sheath) were inserted into the horizontal quartz test chamber through the copper end-plate for monitoring of the substrate temperature, molten metal drop temperature, and the reaction temperatures.

Before each experiment, the substrate and the zinc alloy cube (or wire segment) were ultrasonically cleaned in acetone and the substrate was then carefully slid into the center of the horizontal chamber. According to the static method, a cube of zinc alloy was placed on top of the substrate prior to heating. The sealed chamber was evacuated to a vacuum of 1×10^{-6} Pa and then refilled with the purified Ar-4% H_2 gas. Following the gas purging, the infrared (IR) quartz chamber was heated to the required temperature. The cube of metal was allowed to melt and the wetting behavior between the zinc alloy and the substrate was observed.

For the dynamic sessile drop method, a wire segment of zinc alloy was placed into the quartz tube used for delivering molten zinc to the substrate and this tube was inserted through the copper end-plate into the IR chamber. The chamber was evacuated and refilled in the same manner as for the static test. While the zinc segment in the quartz tube was kept at the cold zone, the IR quartz chamber was heated up to the required temperature. The furnace was allowed to stabilize for 20 minutes before the zinc segment was slowly moved from the cold zone to the hot zone of the furnace where it was allowed to melt and pass through the vertical portion of the delivery tube as a molten drop onto the test substrate. At the end of each experiment, the substrate was removed from the furnace and prepared for examination. Metallographic specimens of the as-received materials and cross-sections of the tested samples were prepared following a standard procedure. The identification of reaction products was conducted using a JEOL 8200 Electron Probe Micro Analyzer (EPMA) with details of the reaction products in the samples examined using a HITACHI 4700 Scanning Electron Microscope (SEM) equipped with an integral Energy Dispersive Spectrometer (EDS).

3 RESULTS

3.1 Wetting and Contact Angle

Illustrating the changes in contact angle and drop geometry with time, Figure 3 shows images of a molten zinc drop on the 316L stainless and MSA2020 substrates during isothermal dwelling at 485°C. The initial contact angle between the 316L substrate and liquid zinc alloy was an obtuse angle ($>90^\circ$) [Figure 3(b)], but was found to gradually decrease to an acute angle ($<90^\circ$) during a hold time of 30 minutes, indicative of the occurrence of reactive wetting [Figure 3(c)]. After the dwelling time was extended to 60 minutes, approximately 50 percent of the molten zinc alloy diffused into the 316L base, significantly changing the geometry of the zinc droplet. At the end of the test (after 120 minutes), almost all the molten zinc permeated into the 316L substrate by diffusion and chemical reaction [Figure 3(d)]. Conversely, the contact angle on the MSA2020 superalloy remained at an obtuse angle throughout the entire 120 minutes dwell time. This final state was considered to represent the obtaining of reactive wetting equilibrium. Differences on the wetting performance between the 316L stainless and MSA2020 base materials are potentially due to the variance in the microstructure and chemical composition of the substrates, leading to the divergence of the reactive wetting kinetics.

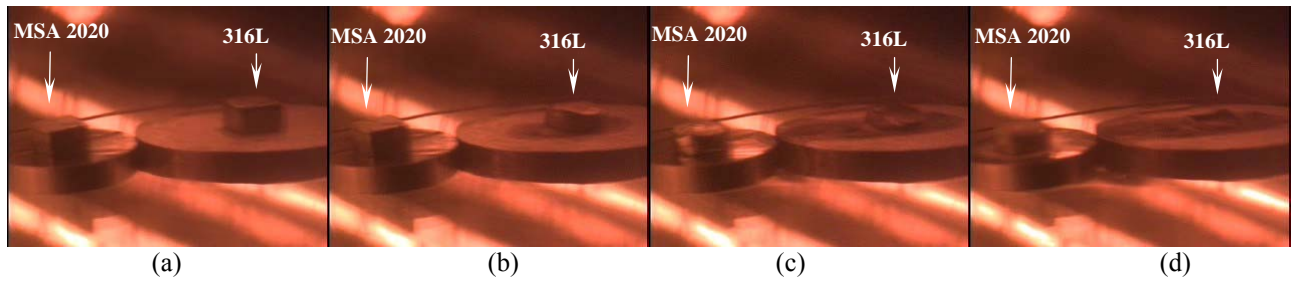


Figure 3: Wetting of MSA200 (left) and 316L stainless steel (right) with the Zn-0.23Al droplet at 485 °C after (a) initial; (b) 10 minutes; (c) 30 minutes; (d) 120 minutes

Four parameters, namely contact angle (CA), drop volume (V), drop base diameter (D), and drop height (H), were analyzed to gain insight into the reactive wetting kinetics. The wetting kinetics could be inferred by combination of the changes in contact angle with the changes in drop size. The change in contact angle characterized by the advance of the triple phase reaction (where the solid substrate, liquid metal, and gaseous experimental environment are in contact) was due to the decrease in the drop height and/or the increase in the drop base diameter. The determinant factor depended on the specific wetting system. From Figure 3, it was observed that the drop volume of both 316L stainless and MSA2020 continuously decreased during the wetting process, minimizing the drop volume present at the end of the wetting tests after 120 minutes. Combining the results obtained after 2 hours at both 465°C and 485°C, shown in Figure 3(d) and Figure 4(a) respectively, it was found that the decrease of the drop height was the dominant sub-stage for the wetting of MSA2020, while the increase in drop base diameter by spreading of the molten zinc overwhelmed the reactive wetting process on 316L stainless.

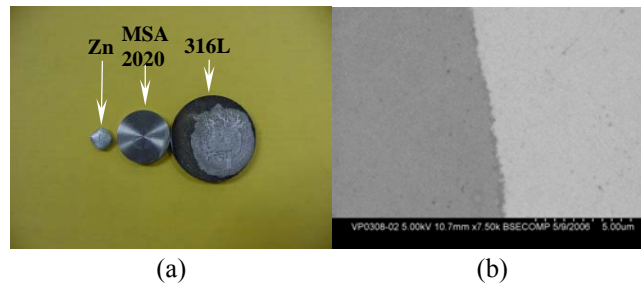


Figure 4: MSA2020 & 316L wetting after 2 hrs at 465 °C (a) Optical view; (b) BSE of cross-sectional of 316L

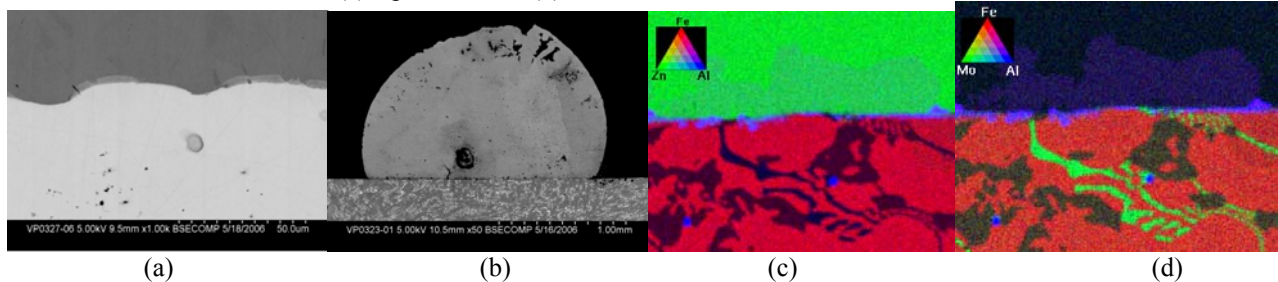


Figure 5: Backscatter micrographs and electron microprobe mapping of wetting with the Zn-0.23Al droplet at 465 °C after 4 hours (a) BSE of 316L; (b) BSE of MSA2020; (c) & (d) EPMA of MSA2020

At 465°C, molten zinc did not wet the MSA2020 after 2 hours, as evident by the solidified drop which easily detached from the substrate after the test without any adhesion [Figure 4(a)]. However, when the dwelling time was extended from 2 hours to 4 hours at 465°C, the molten zinc drop could stick onto the MSA2020 surface more readily, although the contact angle was as large as 145° [Figure 5(b)]. The EPMA analysis showed that a thin Fe-aluminide layer was formed, bonding with the MSA2020 substrate [Figures 5(c) & 5(d)].

Increasing the heating temperature from 465°C to 485°C and subsequently to 500°C, the wetting performance of MSA2020 was studied at higher temperatures. A small molten zinc “pond” was observed around the drop at 485°C, indicating an increase of the drop base diameter [Figure 3(d)]. Analyzing the cross-sectional interface, the contact angle was found to be greater than 90° [Figure 6(a)] despite initiation of reactive wetting and formation of reaction products in the solid base-liquid drop interface [Figure 6(b)]. Additionally a tiny crack was found at the edge of the droplet [Figure 6(a)] probably caused by the coefficient of thermal expansion (CTE) mismatch between zinc and the MSA2020

substrate during cooling. It is hypothesized that the temperature enhancement may decrease the contact angle as a result of enlargement of the droplet on the substrate from greater molten metal fluidity. As an example, the 500°C sessile drop results showed that the contact angle of MSA2020 was reduced to less than 90° [Figure 7(a)] and an interfacial Fe-aluminide intermetallic layer was also observed under such an experimental condition [Figure 7(b)].

On the other hand, for the 316L substrate the molten zinc spread over the base surface [see Figure 4(a)] and the droplet height decreased to nearly zero in all the experiments regardless of the heating temperature (465°C, 485 °C, 500 °C) or dwelling time (1 hr, 2 hrs, 4 hrs). The Fe-aluminide reaction layer was detected by EPMA with varying thicknesses from the cross-sectional microstructures, as shown in Figures 4(b), 5(a), 6(d), and 7(d). Furthermore, reviewing the droplet geometry and macro-bonding, a comparison can be made on the wettability of the base materials, 316L and MSA2020, with molten Zn-0.23wt%Al alloy. As observed in Figures 5 for 465°C-4hours wetting tests and in Figures 6 for 485°C-2hours wetting test, the contact angle of MSA2020 remained obtuse while 316L displayed an acute angle at the above two testing conditions. Conversely, it was determined that 500°C facilitated the wetting activity for both 316L and MSA2020 by reducing the contact angle below 90°C, as shown in Figures 7(a) and 7(c).

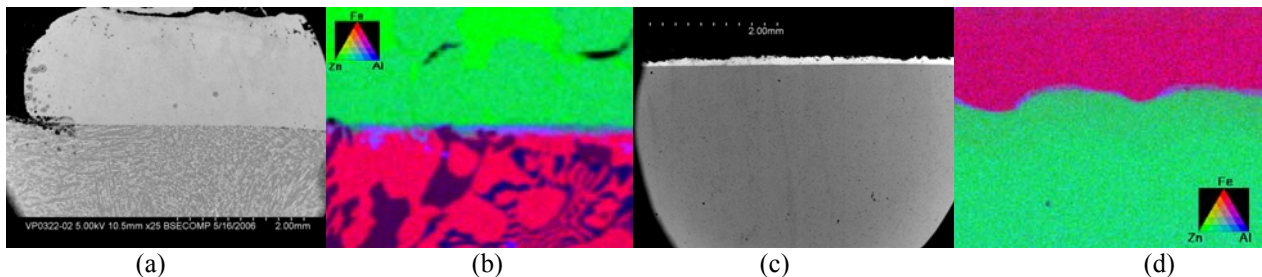


Figure 6: BSE and EPMA mapping of MSA2020 wetting with the Zn-0.23Al droplet after 2 hours at 485°C
 (a) BSE of MSA2020 (b) EPMA of MSA2020 (c) BSE of 316L (d) EPMA of 316L

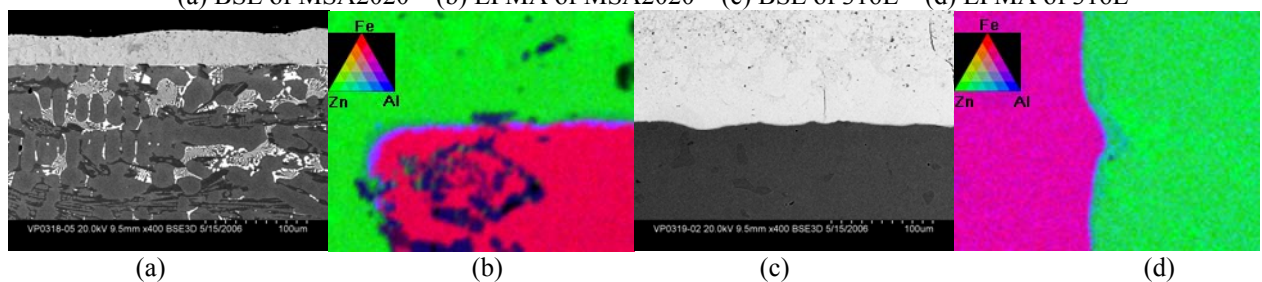


Figure 7: Micrographs of MSA2020 and 316L wetting with the Zn-0.23Al droplet after 1 hour at 500°C
 (a) BSE of MSA2020 (b) EPMA of MSA2020 (c) BSE of 316L (d) EPMA of 316L

It must also be noted that the substrate corrosion reaction could take place even though the contact angle is larger than 90°. Conventionally the contact angle is used to differentiate wetting from non-wetting and a contact angle of 90° or greater generally characterizes a surface as non-wetting. However, this concept is deduced from the macro point of view. Experimental interpretation indicated that the metallurgical reaction may occur even when the liquid droplet and solid base were observed as non-wetting (contact angle is larger than 90°).

3.2 Interfacial Morphology Examination of Reaction Layers

The reaction of 316L and MSA2020 with the Al-containing Zn alloy was found to initiate with the formation of Fe-aluminide layers, regardless of the temperature (ranging 465°C from to 500°C) or time (ranging from 1 hour to 4 hours), and a continuous Fe-aluminide layer was distinctive in both 316L and MSA2020. These Fe-aluminide layers were most likely based on a Fe_2Al_5 structure with some of the Fe sites substituted by Cr, Si, and Mo atoms. δ -phase with diffused Al was also identified as a reaction zone in 316L and MSA2020 in a region receding the Fe-aluminide front layer. The boundaries between the different phases of wetting for MSA2020 were very clear in the EMPA mappings.

As the wetting time at 465°C increased from 2 hours [Figure 4] to 4 hours [Figure 5], the reaction front in the form of an aluminide layer moved further inward from the sample surface and a Zn-rich zone was left behind. As a result, the thicknesses of the reaction layers increased from 0.2 microns [Figures 4(b)] to 3 microns [Figures 5(a)]. Similarly, the increase of the wetting temperature from 465°C to 485°C with the same dwelling time (2 hours) also facilitated the growth of the reaction layer from 0.2 microns [Figures 4(b)] to 5 microns [Figures 6(d)]. Comparing the two substrates under the same testing condition, such as 485°C after 2 hours [Figures 6], the thickness of the reactive layer for 316L stainless (5 microns) was more than double of that for MSA2020 (2 microns), indicating that the reaction driving force of 316L was larger than that of MSA2020. The weaker reactivity of MSA2020 may be explained by its poor affinity to the molten Zn-Al alloy, resulting in a lower diffusion coefficient. In other words, the interfacial reaction force of Zn-Fe

was larger than the reaction of Zn-W/Mo. Neither W nor Mo diffused from MSA2020 into the interface, while Fe did. Figure 7 shows that the result of 500°C-1hour wetting was comparable with that at 485°C-2hours with MSA2020 developing a 2 micron thick intermetallic layer and 316L forming a 5 micron layer.

4 DISCUSSION

4.1 Characterization of Reactive Wetting

The results obtained in this study indicate that 316L stainless and MSA2020 (Fe-based superalloy) react readily with molten Zn-Al alloy but the characteristics of the reactions varied with the alloys and evolved with the reactive wetting times. The findings in the current study imply that the reactive wetting behavior of MSA2020 superalloys in molten Zn-Al alloy is complicated in nature. In addition, the wetting tests prove that the reaction could happen even if the contact angle was observed to be obtuse. Thus, by simply measuring the dimensional or weight changes of the tested samples, the severity of the reaction of an alloy with the test media may be misinterpreted because the results of the measurements depend strongly on how the reaction products (consisting of the residual Zn overlay), the built-up layer and the reaction layer are removed. Some researchers have judged the wettability of a material to molten alloy based only on the contact angle value^(8,9) and such a discernment may significantly underestimate the extent of the reactive wetting because the reaction products may initiate development even with a contact angle larger than 90°. This discovery could, in part, explain discrepancies in the debate of wetting and reaction performance of results reported by different researchers on the materials in molten alloys.

To better understand the reactive wetting kinetics between the liquid zinc alloy and the solid base, it is necessary to discuss the reaction behaviors and the corresponding effects. The influence of the chemical reaction and formation of the Fe₂Al₅ intermetallic layer on the reactive wetting process is not clear. On one hand, the new phase formation promoted wetting of the substrate materials by the chemical reaction, which continuously consumed the reactive elements (Fe, Al, Zn). The propagating chemical reaction assisted the reactive components at a high rate of diffusion since the diffusion was driven by the concentration gradient. The accelerated diffusion facilitated the wetting and shortened the wetting time. On the other hand, the accumulation of the intermetallic compounds at the interface reduced the activity of the reactive wetting. It is perceived that the wettability also depends on the amount of active elements (i.e. Fe) in the tested system. The new intermetallic phases (Fe₂Al₅) accumulated at the interface between the molten zinc alloy and the solid base, partially covering the reactive sites and requiring the Fe to slowly diffuse across this aluminide layer. From this perspective, the Fe₂Al₅ reaction layer possessed effects similar to an inhibition layer, where consumption of the Al by the Fe₂Al₅ intermetallic layer depleted the reactive Al at the substrate/ zinc interface.

4.2 Mechanism of Reactive Wetting

It was observed from EPMA mapping that Al is the most corrosive ingredient in the molten alloy because it reacts with transition metals and forms aluminides with relatively low free energies of formation. The reaction of 316L with the Zn-Al bath would obviously form Fe-aluminides at the initial stages. A similar reaction took place in the case of MSA2020, but required longer time than 316L for inciting the reaction before the energy barrier was overcome.

The formation of the Zn-rich reaction zones behind the moving reaction fronts in the alloys created chemical compositions of the reaction zones which were quite different. The Zn-rich layer in the 316L contained close to 95% Zn and only 0.8% Al and is likely based on the δ -phase (Zn₁₀M). Conversely, the reaction zones formed in MSA2020 contained considerable amounts of Al (10.4%). In addition, EPMA mapping did not detect any Mo in the reaction zone, minimizing the likelihood of Mo-aluminide formation. This result differs from previous research on another Fe-based superalloy, T-500M, where a large amount of Mo₃Al₈ was found in the reaction zone⁽²⁾. This variance is possibly due to the difference in chemical composition of the solid solution phases in these alloys, where T-500M contained an appreciable amount of Mo while only a limited amount of Mo was added to MSA2020.

For both 316L stainless and MSA2020 superalloy, the reactive wetting could be explained in three steps. It started with the wetting and diffusion of the molten Zn-Al to the solid base, followed by the conversion of the Fe solid solution phase into an Fe-aluminide of the matrix components. Subsequently, this aluminide layer was converted into the δ -phase (Zn₁₀M) in 316L and Zn-rich Al-Fe intermetallic phases in MSA2020. The relatively stable intermetallic phases containing Mo, W and Cr were left undisturbed due to their dissension of molten zinc alloy. Apparently, such a three-step process allows the early participation of Zn in reactive wetting and, hence, is kinetically favored.

4.3 Alloying Elements Effects and Other Influence Factors

It was concluded that the wettability was significantly affected by key factors such as alloying elements, the solid base density, and roughness of the substrate materials. For the MSA2020 superalloy, the alloying constituents segregating on the surface would cover part of the free iron surface and subsequently reduce wettability of molten zinc and aluminum with Fe. Moreover, introduction of Mo-W-Cr intermetallic phases at the solid-liquid interface offset the roughness effect on wetting, curving the interfacial boundary. The liquid zinc initially reacted with the Fe solid solution, which was located in the valley between those spattered intermetallic phases. The same conclusion was made in the case of Cu wetting by PbSn solder.^(10,11) The difference in the roughness of the Cu₆Sn₅ intermetallic in the inner regions and at the reaction band at the edge of the solder imparted great effect on the wettability.

Moreover, the addition of alloying elements to the MSA2020 superalloys to promote the formation of Mo-W-Cr intermetallic phases apparently improved the resistance of the alloy to the reactive wetting by molten Zn-Al alloy. Results obtained in this study revealed that the phases containing Mo-W-Cr were more stable than the Fe solid solution phases, and these phases were not attacked by molten zinc alloy during the reactive wetting process. Containing Mo, W and Cr of significant amount, MSA2020 displayed better wetting resistance than 316L which contains Cr, Ni and Mo. Further investigation is warranted to explore the mechanisms and to verify the applicability of MSA2020 superalloy as a galvanizing pot hardware material.

The surface roughness was another important factor influencing the wettability. Since all the specimens were polished under the same conditions, the effect caused by the surface roughness was assumed to be negligible compared with the interfacial reaction which contributed more to the wetting dynamics. It is postulated that if the substrate materials were manufactured with a more porous structure, the solid base would adsorb the liquid phase, accelerating the wetting process. However, considering that the base materials, 316L stainless and MSA2020, were dense and compact, the decrease in contact angle was not a consequence of adsorption effects.

5 CONCLUSIONS

In order to explore the mechanism of reactive wetting occurring between zinc alloy and steel/superalloy substrates, the wetting behavior of a GI zinc alloy (Zn-0.23Al) was investigated using the sessile drop technique. A link can be made between the wettability and the activity for zinc and aluminum to react with metallic iron. It was found that Fe-aluminide, based on the Fe_2Al_3 phase, formed in the reaction layer on 316L stainless steel and MSA2020, an Fe-based superalloy. Alloying elements Mo/W/Cr added to the MSA2020 superalloy significantly improved the wetting resistance to molten zinc. Since the current reactive wetting theory suggested that the first intermetallic compound formed during the wetting reaction could influence the wetting properties, the reaction of the base alloy and molten zinc droplet was discussed. Several findings were observed:

- (1) MSA2020 superalloy possessed better wetting resistance than 316L in contact with the molten zinc alloy at test temperatures of 465°C, 485°C, and 500°C.
- (2) The contact angle of MSA2020 remained at an obtuse angle throughout the wetting tests of 4 hours at 465°C and 2 hours at 485°C. However, the contact angle of MSA2020 wet by the molten zinc alloy dropped to an acute angle when the temperature was increased to 500°C. Conversely, a molten zinc film started to spread over the 316L surface in the first half hour of dwelling at 465°C. Reactive wetting became more severe when the temperature was increased.
- (3) The surface reaction was found to initiate even though the liquid droplet and solid base were observed as non-wetting (contact angle larger than 90°).
- (4) The alloying constituents (W, Mo, Cr) in MSA2020 stably segregating on the surface reduced the wettability by molten Zn-Al by covering the reactive sites on the solid-liquid interface.

ACKNOWLEDGEMENTS

The authors would like to thank Metallurgical Systems Division of Pyrotek Inc. for their cooperation to publish these results. Thanks are due to Wheeling-Nisshin, Inc. who helped with supplying the galvanizing zinc. We acknowledge the contributions of Randy Parton, Randy Howell, and Donny McInturff of ORNL in support of the experimental execution described in this paper. The efforts of Mingyang Gong in reviewing this document are also appreciated. This research was sponsored by the U.S. Department of Energy, Office of Energy Efficiency and Renewable Energy, Industrial Technologies Program, for the U.S. Department of Energy under contract DE-FC36-04GO14038 and was supported by the Industries of the Future-West Virginia.

REFERENCES

- 1) K. Zhang, N.-Y. Tang: Galvatech '04 Conference Proceedings, Chicago, (2004), 617 – 627.
- 2) K. Zhang, N.-Y. Tang: Materials Science and Technology, 20(2004), 739-746
- 3) M.S. Brunnock, R.D. Jones, G.A. Jenkins, and D.T. Llewellyn: Ironmaking and Steelmaking, 24(1997), 40-46
- 4) Kiyoshi Nogi: Proc. of Result Presentations for International Joint Research Grant Program Proposals, NEDO, (2005), H-17
- 5) L. Bordignon: ISIJ international, 41(2001), 168-174
- 6) M.-L. Giorgi, M. Zaidi, J.-B. Guillot. North American GAP Program Review Meeting, (2005), 40
- 7) B. Gay, A. Piccinin, and M. Dubois: Proc. Galvatech '01, Brussels, (2001), 262 – 269
- 8) J.E. Kelley, H.M. Harris: Journal of Testing and Evaluation, 2(1974), 40
- 9) A. Salehi, S. Tsai, V. Pawar, J. Sprague, G. Hunter, et. al: Key Engineering Materials, 309-311(2006), 1199-1202
- 10) A.S. Zuruzi, C.-H. Chiu, S.K. Lahiri, and K.N. Tu: Journal of Applied Physics, 86(1999), 4916-21
- 11) A.J. Sunwoo, J.W. Morris, and G.K. Lucey: Metallurgical Transactions A, 23(1992), 1323-32